

Articles

Ab Initio and Crystal Structures of (*E,E*)-1,4-Diphenylbutadiene: A New Type of Arene–Arene Double T-Contact and an Interesting Interlayer Cooperation Involving Diastereoisomeric Contacts[†]

Rainer Glaser,* Laxma R. Dendi, Nathan Knotts, and Charles L. Barnes

Department of Chemistry, University of Missouri-Columbia, Columbia, Missouri 65211

Received January 16, 2003; Revised Manuscript Received February 24, 2003

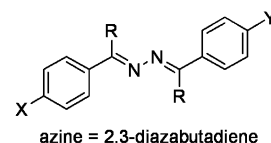
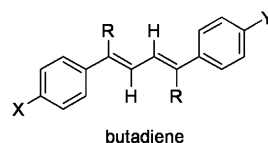
Ⓜ This paper contains enhanced objects available on the Internet at <http://pubs.acs.org/crystal>.

ABSTRACT: The title compound 1,4-(*E,E*)-diphenylbutadiene crystallizes in the space group $P2_1/n$, and the structure contains three independent molecules A–C with modest twisting about the C–Ph bonds. Each molecule engages in two double face-to-face contacts and in four double T-contacts of a new type. These arene–arene interactions form two-dimensional layers that are stacked in the third dimension. In the new double T-contact, both arenes of each laterally off-set spacer-connected diarene serve as faces or edges in each contact. The occurrence of either one independent molecule (A) in two orientations (+A and –A) or of two independent molecules (B and C) results in two diastereoisomeric double T-contacts in each layer. Molecule A is asymmetric and forms enantiomeric (–A+A) and (–A'+A') layers. The alternation between layers with different pairs of diastereoisomeric double T-contacts allows for reduced surface-matching and better van der Waals interactions between the surfaces of the –A+A (–A'+A') layers and the BC layers.

Introduction

Highly anisotropic materials are interesting for a variety of reasons, and we are specifically interested in the design and realization of highly anisotropic materials with polar order.¹ A relatively modest molecular dipole moment is a fundamental prerequisite for the parallel alignment of polar materials.² We have focused on unsymmetrically substituted 1,4-diphenyl-2,3-diaza-butadienes ($X \neq Y$) because the azine spacer functions as a conjugation stopper and provides quadrupolarity. We prepared and reported three acetophenone azines ($R = \text{Me}$, $X = \text{OPh}$, $Y = \text{Hal}$)³ with near-perfect dipole parallel-alignment and, more recently, we also accomplished the fabrication of three perfectly dipole parallel-aligned acetophenone azines ($R = \text{Me}$, $X = \text{OPh}$, $Y = \text{Hal}$).⁴ As part of the deep analysis of these prototypes, one line of research aims at supporting the assumptions that guided the design of the azine materials. This involves the theoretical and experimental

characterization of the electronic structure of azines,^{5,6} and it also involves probing the properties of the related unsymmetrical 1,4-diphenylbutadienes. All of these efforts are directed at a better understanding of the interplay between intramolecular features and intermolecular bonding in the crystal with a focus on arene–arene interactions.⁷ In this context, we are reporting here on the crystal structure of the parent 1,4-diphenylbutadiene (**1**, $R = X = Y = \text{H}$).



More than half a century ago, unit cells of crystals of 1,4-diphenylbutadiene were reported, and these reports suggest the occurrence of at least three polymorphs. In 1930, Hengstenberg and Kuhn reported unit cell dimensions of monoclinic crystals,⁸ and in 1953, Drenth and Wiebenga reported a second monoclinic and an orthorhombic structure.⁹ The lattice constants of the structure we report here are in close agreement with the data

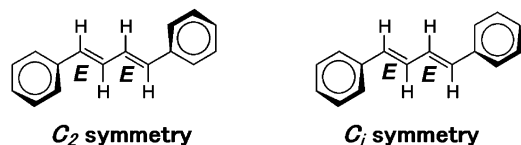
[†] Part 18 in the series "Stereochemistry and Stereoelectronics of Azines and Dienes."

* To whom correspondence should be addressed. Telephone: (573) 882-0331, Facsimile: (573) 882-2754. E-mail: glaserr@missouri.edu.

Table 1. Lattice Constants for **1**

parameter	Hengstenberg & Kuhn 1930	Drenth & Wiebenga 1953		this work
	I	II	III	III
crystal preparation	monoclinic glacial acetic acid	orthorhombic III, 100° below mp.	monoclinic EtOH or CHCl ₃	monoclinic EtOH diff into CHCl ₃
<i>a</i> (Å)	7.71	8.89	5.86	5.8106
<i>b</i> (Å)	11.70	8.22	7.66	7.533
<i>c</i> (Å)	13.41	12.68	53.1	53.367
β (°)	97.	90.	91.	91.067
density (calc, mg/mm ³)	1.138	1.124	1.142	1.173
molec per unit cell	4	4	8	8

by Drenth and Wiebenga (Table 1). We begin with a report of the results of ab initio studies of 1,4-diphenylbutadiene to provide pertinent background information about intrinsic structural preferences.



Materials and Methods

Ab Initio Computations.¹⁰ Optimizations were carried out using restricted Hartree–Fock theory (RHF), second-order Møller–Plesset perturbation theory (MP2), and the B3LYP method of density functional theory. B3LYP denotes a three-parameter hybrid density functional that combines Becke's exchange functional with the correlation functional by Lee, Yang, and Parr. All electrons were included in the active space of the perturbation calculation, MP2 (full). The structure of **1** was completely optimized without any symmetry constraints (*C*₁, 84 degrees of freedom) with appropriate initial geometries and *C*₂, *C_i*, or *C*_{2h} symmetry resulted. In cases in which *C*₂ or *C_i* structures were minima the planar *C*_{2h} structure also was optimized (29 degrees of freedom). To ascertain the preference for either of the twisted structures over the planar structure, single point calculations were carried out using coupled cluster theory with single and double excitations, and the frozen core approximation was employed in these calculations, CCSD(fc). The basis sets 6-31G* (A) and 6-311G** (B) were employed for structure optimizations. The CCSD(fc) calculations were performed with the 6-31G* basis set; CCSD(fc) calculations on molecules of this size with the fully polarized triple- ζ basis set are not possible even with modern hardware. However, we were still able to perform the third- and fourth-order perturbation calculations, MP3 and MP4, with the larger basis set. All calculations were carried out with Gaussian 98¹¹ on a cluster of Compaq ES45 alphaservers. Pertinent energy and structural data are summarized in Tables 2 and 3. Cartesian coordinates of the MP2(full)/6-311G** optimized structures are provided as Supporting Information.

Crystallization and Crystallography. 1,4-Diphenylbutadiene was purchased from Aldrich Chemicals. Crystals were grown by slow diffusion of ethanol into a solution of **1** in chloroform. The crystallographic data are given in Tables 4 and 5, and details are provided as Supporting Information.

Results and Discussion

Potential Energy Surface Analysis of (E,E)-1,4-Diphenylbutadiene. At the RHF level, the minimum structures are predicted to be *C_i* and *C*₂ symmetric with a C=C–C=C dihedral angle τ of exactly or very close to 180°, respectively, and a significant rotation ϕ of the phenyl groups (about 14°). Forcing planarity comes at no cost; the planar structure is less than 0.1 kcal/mol less stable than either of the twisted structures (Table

Table 2. Total and Relative Energies^a

parameter	<i>C_i</i>	<i>C₂</i>	<i>C_{2h}</i>
6-31G*			
<i>E</i> (RHF)	−614.02830	−614.02831	−614.02820
<i>E</i> (MP2(full))	−616.12497	−616.12498	−616.12458
<i>E</i> (B3LYP)	−618.11742	−618.11742	−618.11735
<i>E</i> (MP3(fc))	−616.11162	−616.11164	−616.11116
<i>E</i> (MP4(fc))	−616.13021	−616.13022	−616.12961
<i>E</i> (CCSD(fc))	−616.13285	−616.13287	−616.13221
<i>E</i> _{rel} (RHF)	0.06	0.07	
<i>E</i> _{rel} (MP2(full))	0.24	0.25	
<i>E</i> _{rel} (B3LYP)	0.04	0.04	
<i>E</i> _{rel} (MP3(fc))	0.29	0.30	
<i>E</i> _{rel} (MP4(fc))	0.37	0.38	
<i>E</i> _{rel} (CCSD(fc))	0.40	0.41	
6-311G**			
<i>E</i> (RHF)	−614.15845	−614.15845	−614.15839
<i>E</i> (MP2(full))	−616.64970	−616.64972	−616.64903
<i>E</i> (B3LYP)	−618.26844	−618.26844	−618.26834
<i>E</i> (MP3(fc))	−616.41382	−616.41384	−616.41325
<i>E</i> (MP4(fc))	−616.42608	−616.42610	−616.42549
<i>E</i> _{rel} (RHF)	0.04	0.04	
<i>E</i> _{rel} (MP2(full))	0.42	0.43	
<i>E</i> _{rel} (B3LYP)	0.06	0.06	
<i>E</i> _{rel} (MP3(fc))	0.35	0.37	
<i>E</i> _{rel} (MP4(fc))	0.37	0.38	

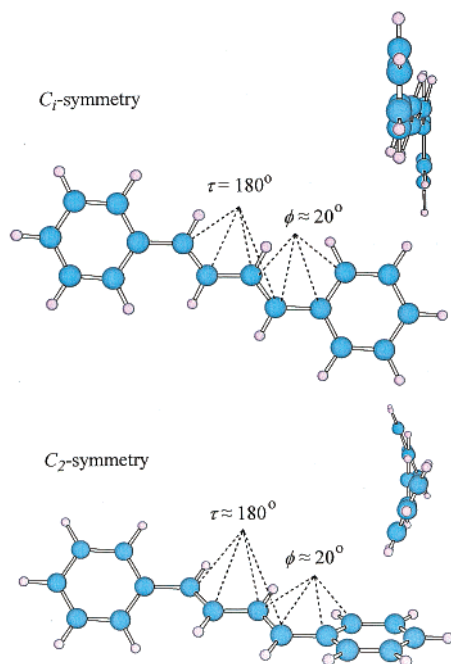
^a Total energies in atomic units and relative energies in kcal/mol. Relative energies specify the preference of the twisted structures relative to the planar structure.

2). Using the B3LYP density functional method, unconstrained optimization starting with twisted and chiral structures resulted in de facto *C*_{2h} structures using both basis sets. The energies of these structures are slightly lower (less than 0.1 kcal/mol) than the energies of the same structures optimized with the symmetry constraint to *C*_{2h} symmetry. As with the RHF level, at the MP2(full) level the minimum structures again are predicted to be *C_i* and *C*₂ symmetric with a C=C–C=C dihedral angle τ that is exactly or essentially 180° and significant rotations ϕ of the phenyl groups (narrow range of 22–25°). In contrast to the RHF results, however, forcing planarity does come at a small cost at the MP2(full) level and the planar structure is about 0.3–0.4 kcal/mol less stable than the twisted structure.

The two correlated methods thus differ as to whether the gas-phase structure of **1** prefers planarity (as suggested by B3LYP) or twisted phenyl groups (as suggested by MP2). One way to resolve this discrepancy involves the calculation with more accurate electron correlation methods, and we employed coupled cluster theory for this purpose. The MP2 and CCSD methods both estimate correlation effects by consideration of single and double excited configurations. While MP2 estimates their contributions based on a perturbation scheme, the correlation coefficients are variationally optimized in the CCSD method. We carried out CCSD

Table 3. Major Structural Parameters^a at MP2(full)/6-31G* and MP2(full)/6-311G**

parameter	MP2(full)/6-31G*			MP2(full)/6-311G**		
	C_i	C_2	C_{2h}	C_i	C_2	C_{2h}
C8–C9	1.441	1.441	1.442	1.444	1.443	1.442
C8=C7	1.354	1.354	1.357	1.356	1.356	1.357
C7–C1	1.461	1.462	1.461	1.463	1.463	1.461
C1=C2	1.406	1.405	1.409	1.407	1.408	1.409
C2=C3	1.392	1.392	1.394	1.394	1.395	1.394
C3=C4	1.397	1.396	1.400	1.400	1.400	1.400
C4=C5	1.394	1.394	1.397	1.398	1.398	1.397
C5=C6	1.393	1.393	1.395	1.395	1.395	1.395
C6=C1	1.405	1.404	1.408	1.407	1.407	1.408
C9–C8–C7	123.4	123.4	123.0	123.4	123.4	123.0
C8–C7–C1	125.9	125.9	127.0	125.6	125.6	127.0
C7–C1–C2	122.5	122.5	123.2	122.3	122.2	123.2
C7–C1–C6	119.3	119.2	118.7	119.4	119.4	118.7
C10=C9–C8=C7, τ	180.0	180.0	180	180.0	178.7	180
C8–C7–C1–C2, ϕ	22.0	22.0	0	24.0	24.3	0

^a In Å and deg.**Figure 1.** Molecular models of the MP2(full)/6-311G** optimized C_i and C_2 symmetric structures of **1**.

⊗ 3D molecular models of the optimized structures: ⊗ C_i , ⊗ C_2 , ⊗ C_{2h} at RHF/6-31G*; ⊗ C_i , ⊗ C_2 , ⊗ C_{2h} at RHF/6-311G**; ⊗ C_i , ⊗ C_2 , ⊗ C_{2h} at MP2/6-31G*; and ⊗ C_i , ⊗ C_2 , ⊗ C_{2h} at MP2/6-311G** in PDB format are available.

calculations for the C_i , C_2 , and C_{2h} symmetric MP2-optimized structures using basis set A. The CCSD energy calculations confirm the MP2 results. The higher-order perturbation calculations with the larger basis show no basis set effect. Hence, our computations suggest that the gas-phase structures of 1,4-diphenylbutadiene is *s-trans* about the central bond with $\tau = 180^\circ$,¹² features a phenyl twist of $\phi \approx 20^\circ$, that the twists leading to C_i and C_2 symmetry are essentially isoenergetic, and that planarization requires less than 0.5 kcal/mol. The MP2/6-311G**-optimized C_i and C_2 structures are displayed in Figure 1. Major structural parameters of **1** are summarized in Table 3, and it can be seen that basis set effects are small.

Crystal Structure of (E,E)-1,4-Diphenylbutadiene. Crystallographic information is presented in Table

Table 4. Crystal Data and Structure Refinement of **1**

compound	$C_6H_5-CH=CH-CH=CH-C_6H_5$
color/shape	colorless/plates
chemical formula	$C_{16}H_{14}$
formula weight	206.27
temperature (K)	173(2)
crystal system	monoclinic
space group	$P2_1/n$
a (Å)	5.8106(12)
b (Å)	7.5333(15)
c (Å)	53.367(11)
β (°)	91.067
volume (Å ³)	2335.6(8)
Z	8
density, calc (mg/mm ³)	1.173
absorption coefficient (mm ⁻¹)	0.066
diffractometer/scan	Bruker SMART CCD area detector
θ range for data collection (°)	2.73–21.97
reflections measured	8055, 8793 reflections in full θ range
independent/observed reflections	2796 [$R_{int} = 0.0490$]/2127
data/restraints/parameters	2796/0/290
extinction coefficient	0.0015(9)
goodness of fit on F^2	1.156
final R indices [$I > 2\sigma(I)$]	$R_1 = 0.0913$, $\omega R^2 = 0.1937$
R indices (all data)	$R_1 = 0.1149$, $\omega R^2 = 0.2047$

4. The crystals belong to the $P2_1/n$ space group with cell parameters $a = 5.8106(3)$, $b = 7.5333(3)$, $c = 53.367(11)$ Å, and $\beta = 91.067^\circ$. ORTEP II and PLUTO diagrams are shown in Figures 2 and 3.

The crystal structure of **1** contains three independent molecules A, B, and C (Figure 2). Molecule A is asymmetric and is slightly twisted about the central C8–C9 bond with $\tau_C = 177.2^\circ$ and phenyl twist angles $\phi_{A1} = 3.9^\circ$ and $\phi_{A2} = 2.7^\circ$. We always define the phenyl twist angle as shown in Figure 1, that is, as the dihedral angle C=C–C–C_{ortho}. For each molecule A the angles ϕ_{A1} and ϕ_{A2} have opposite sign, that is, the phenyl twists are C_i -like. Molecules B and C are C_i -symmetric, and hence they are perfectly *s-trans*, $\tau_B = \tau_C = 180^\circ$. The phenyl twists in molecules B and C are $\phi_B = 12.8^\circ$ and $\phi_C = 0.8^\circ$, respectively.

In Table 5, the major structural parameters of molecules A, B, and C are summarized, and there are no structural manifestations of varying conjugation as a function of the ϕ dihedral angle. C is planar for all practical purposes, and A is almost planar and their

Table 5. Comparison of Major Structural Parameters^a in A, B, and C

bond	A	B	C	average
C8–C9	1.431(7)	1.453(9)	1.433(9)	1.437 ± 0.016
C8=C7	1.328(7)	1.352(7)	1.356(7)	1.340 ± 0.016
C9=C10	1.324(7)			
C7–C1	1.461(7)	1.469(6)	1.461(6)	1.463 ± 0.006
C10–C11	1.461(7)			
C1=C2	1.402(7)	1.397(6)	1.411(6)	1.398 ± 0.004
C11=C12	1.385(7)			
C2=C3	1.362(7)	1.384(6)	1.379(7)	1.374 ± 0.010
C12=C13	1.372(7)			
C3=C4	1.375(7)	1.371(7)	1.393(7)	1.382 ± 0.011
C13=C14	1.392(7)			
C4=C5	1.386(7)	1.383(7)	1.368(7)	1.380 ± 0.006
C14=C15	1.383(7)			
C5=C6	1.375(7)	1.385(7)	1.365(7)	1.369 ± 0.016
C15=C16	1.374(7)			
C6=C1	1.404(7)	1.388(6)	1.386(7)	1.394 ± 0.010
C16=C11	1.398(7)			
C10=C9–C8=C7, τ	177.1(6)	180.0	180.0	
C8–C7–C1–C2, ϕ_1	2.7(8)	–12.7(8)	0.8(8)	
C9–C10–C11–C12, ϕ_2	–3.9(9)	12.7(8)	–0.8(8)	

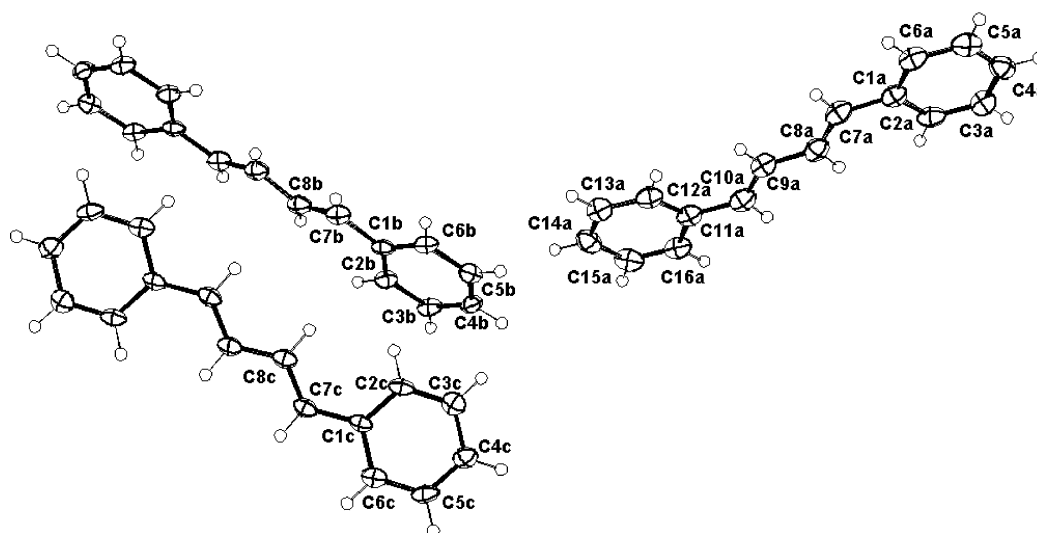
^a In Å and degrees.

Figure 2. ORTEP drawing of 1,4-diphenylbutadiene 1.

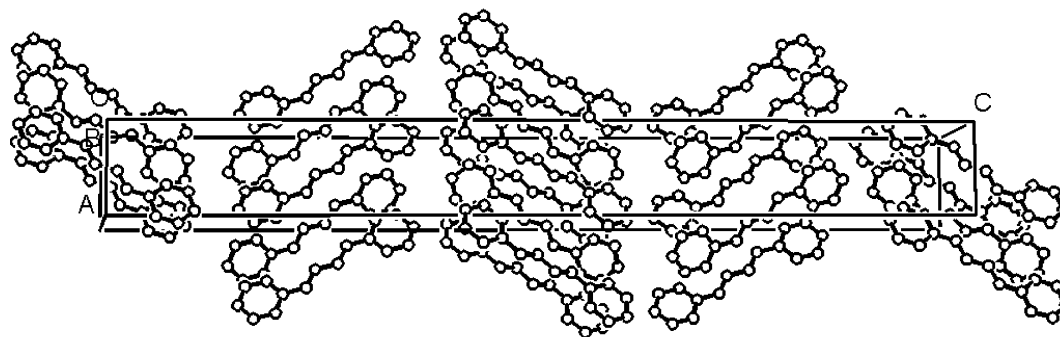


Figure 3. PLUTO drawing of the crystal packing of 1,4-diphenylbutadiene 1.

C7–C1 bonds of 1.361 Å are the same. The nonplanar structure B shows a slightly elongated Ph–C bond of 1.469 Å and a slightly elongated C8=C7 bond length as compared to C. However, these observations do not indicate conjugation effects in light of the fact that the almost planar and the planar structures A and C differ the most in the C8=C7 double bond length, by about

0.03 Å. Clearly, these variations are inconsistent with conjugation effects and must be caused by intermolecular packing.

A comparison of the structure of 1 to the structure of styrene would be instructive, but the structure of pure styrene has not been determined as yet.¹³ Only one structure of a cocrystal with an ordered styrene was

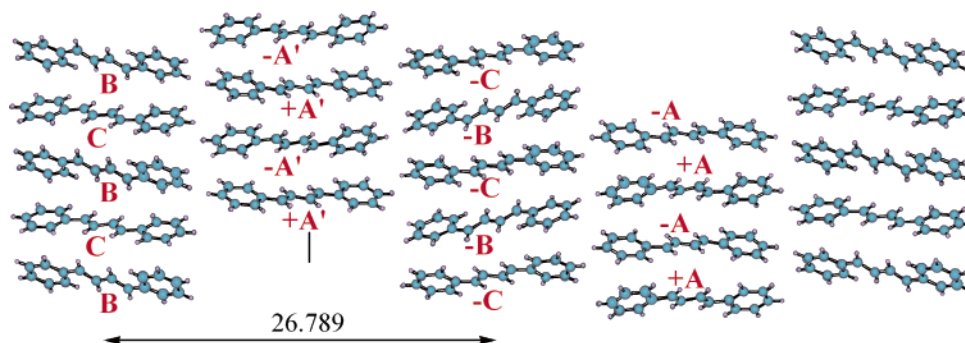


Figure 4. Chem3D representation of the crystal packing of 1,4-diphenylbutadiene **1**, viewed down the diagonal of the **ab**-plane with the *c*-axis aligned horizontally.

Ⓢ A 3D rotatable crystal structure of **1** in PDB format is available.

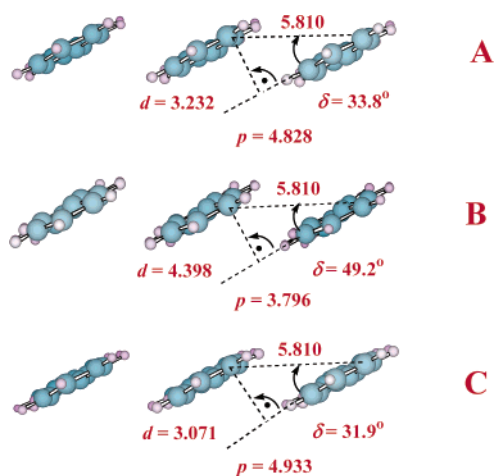


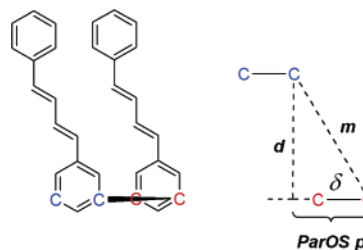
Figure 5. Columns of molecules A, B, and C in the crystal of 1,4-diphenylbutadiene **1**. The molecules in each column interact with each other by way of double face-to-face arene–arene contacts (ff|ff).

Ⓢ 3D rotatable images of columns of molecules Ⓢ A, Ⓢ B, and Ⓢ C in PDB format are available.

reported, and, unfortunately, the styrene in this cholic acid styrene clathrate features a much too short C=C double bond length of 1.189 Å and a much too large vinylic C–C–C angle of 144.2°.

The crystal structure of **1** is a layered structure (Figure 3). The two-dimensional layers contain the molecules with their long axis (almost) perpendicular to the directions of layer extension, and the thickness of the layers thus is roughly equal to the length of the molecule (ca. 14 Å). Figure 4 shows that the layers contain columns of molecules A, A', B, and D, and Figure 5 shows that these columns allow for parallel-displaced double face-to-face interactions. Each molecule is involved in two double face-to-face contacts, and each molecule serves as a “double-face”. For brevity, we characterize such double arene–arene contacts by specification of the type of coordination mode (“f” for face or “e” for edge) of the two arenes in each molecule. Each molecule is characterized as (ee), (ff), (ef), or (fe), and a “double arene–arene contact” is characterized by the two pairs that characterize the two molecules, and these are separated by a vertical bar. Hence, the “double face-to-face contacts” in Figure 5 are of the (ff|ff) type. We are characterizing the parallel off-set (ParOS, *p*) and the stacking distance (SD, *d*) between the faces of the

molecules as described by eqs 1 and 2 based on the measurements of the distance *m* and the angle δ . Molecules B differ greatly from A and C as far as the phenyl twist angles ϕ are concerned, and this has consequences for the column geometry. The columns built by B feature a δ angle that is larger than for A and C, and, consequently, the off-set value *p* is shorter for B than for A and C and the distance *d* is markedly larger for B than for A and C.



$$\cos(\delta) = p / m \quad (\text{eq. 1})$$

$$\sin(\delta) = d / m \quad (\text{eq. 2})$$

The columns of enantiomers A and A' form separate chiral layers. Within each of these A and A' layers, the *molecular orientation* differs in alternating columns. We designate as +A and –A molecules of the *same* chirality that have been flipped around their short axis. The columns of B and C molecules in one layer, on the other hand, do not show alternation of molecular orientation. Every B molecule in a BC layer has the same sign of ϕ_B on the “left” and the opposite sign of ϕ_B on the “right”, while these signs are reversed in the following (–B–C) layer.

Rotation of the respective crystal segments shown in Figure 4 around the *vertical* axis results in the side-views of the BC and AA layers shown in Figure 6. The figure illustrates well that each benzene molecule is surrounded by four benzene molecules in such a way that four edge-to-face or T-contacts result. Since each 1,4-diphenylbutadiene contains two benzene rings, both benzene rings of one molecule interact with both benzene rings of an adjacent molecule in an edge-to-face fashion and a “double T-contact” occurs. Using blue lettering in Figure 6, we emphasize the environment of one B molecule. Each molecule B engages in four double T-contacts with molecules C and vice versa. Likewise,

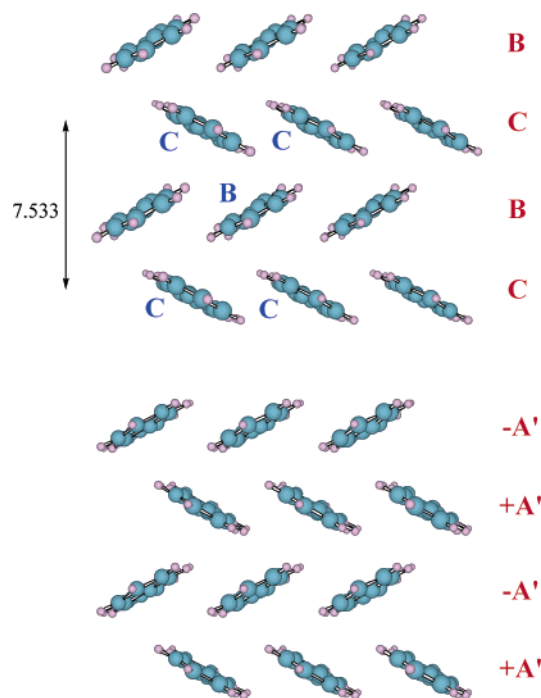
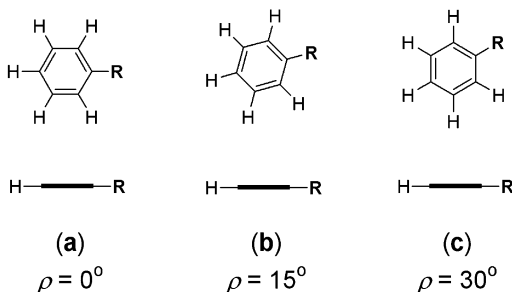


Figure 6. Views of the BC and AA layers of 1,4-diphenylbutadiene **1** viewed down the long molecular axis show that each molecule engages in four double T-contacts.

Ⓢ 3D rotatable images in PDB format of the Ⓢ BC and Ⓢ AA layers in the crystal structure of **1** are available.

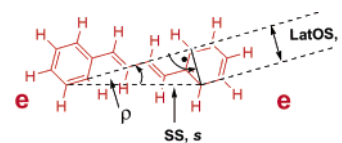
each A engages in four double T-contacts with proximate A molecules.



Detailed theoretical studies of benzene dimer show a variety of structures, and many of these are close in energy.¹⁴ Double T-contact formation reduces the options because each arene–arene interaction must allow for the other. One way to realize a double T-contact involves true edge-to-face coordination, that is, one edge of benzene is parallel aligned with the face of the other benzene, option (a). In options (b) and (c), the edge is no longer parallel with the plane of the facing benzene, and in option (c) one C–H bonds points toward the face of the benzene. The type of rotation can be described by the angle ρ . In acetophenone azines, we found a dominance of C_2 -causing twisting, both of the phenyl groups and of the central N–N bond, and this twisting offers the advantage of realizing an excellent double T-contact in which one benzene functions as the face and one functions as the edge. Importantly, this type of double T-contact can be accomplished perfectly well with very small ρ -angles. The structure of 1,4-diphenylbutadiene offers a different double T-contact for the first time. In this new type of double T-contact both

benzenes of one molecule function as faces and both benzenes of the other molecule function as edges in the two T-contacts. Each molecule is involved in four double T-contacts and the molecule serves as a “double-edge” (Figure 6, B with upper right C and bottom left C) or a “double-face” (with upper left C and lower right C) synthon in two contacts. Using the abbreviations above, the commonly observed azine double T-contacts is of the (fe|ef) type and the double T-contacts in the present structure are (ff|ee) and (ee|ff). Schematic representations of these double T-contacts are shown in Figure 7.

A prerequisite for an (ff|ee) double T-contact is a spacer that causes “lateral off-set” (LatOS, l). Each benzene has a local rotational axis and a LatOS spacer is one that causes these two local rotational axes to be noncollinear. No lateral off-set requires $\rho = 0$ and the value for ρ depends on the lateral off-set l caused by the spacer and the length of the synthon spacing (SS, s). This is illustrated by comparison of the diene and the diene spacers in the center of Figure 7 and the relation between ρ , l , and s is given by eq 3.



$$\sin(\rho) = l / s \quad (\text{eq. 3})$$

It is clear from Figure 6, that there are two (ee|ff) contacts in the BC layers; B is the (ee) part in one and the (ff) part in the other. In the layers of the A or A' molecules, there *also* are two diastereoisomeric contacts because of the alternating orientation of the chiral molecules in the layers. If the A molecules would not be chiral or if all A (or A') molecules in one layer were chiral but had the same orientation, then there would be just one type of (ee|ff) contact, and each molecule would be involved in this contact twice as the (ee) and twice as the (ff) component. Since A is chiral, it has the ability to occur in two orientations and actually does occur in these two orientations, and two diastereoisomeric (ee|ff) contacts are realized in which A is (ee) or –A is (ee) and vice versa. The structures to the right in Figure 7 are diastereoisomers only if the molecules are chiral (half 1 and 2 differ) and their orientations differ (top is rotated).

The four unique (ff|ee) double T-contacts in the crystal structure of **1** are shown in Figure 8. The dimers are displayed in such a fashion that the (ff) molecule is on the bottom and the arene on the left is in the foreground. We measured the values of s and ρ for these pairs and determined the effective off-set via eq 3, and these values are given in Figure 8. The values of ρ and s typically are 12–13° and close to 9 Å, respectively, and the computed off-set of the diene spacer in **1** is about $l = 2$ Å.

There is one more important off-set value to characterize the double T-contacts, and this is the longitudinal off-set between the (ff) and (ee) molecules along their long axes. We determine this off-set l' via eq 4 based on the measurements of the distance s' between the C_{para} atom and the angle ω between the $C_{\text{para}}-C_{\text{ipso}}$ direction of the (ff) molecule and C_{para} of the (ee) molecule. In most

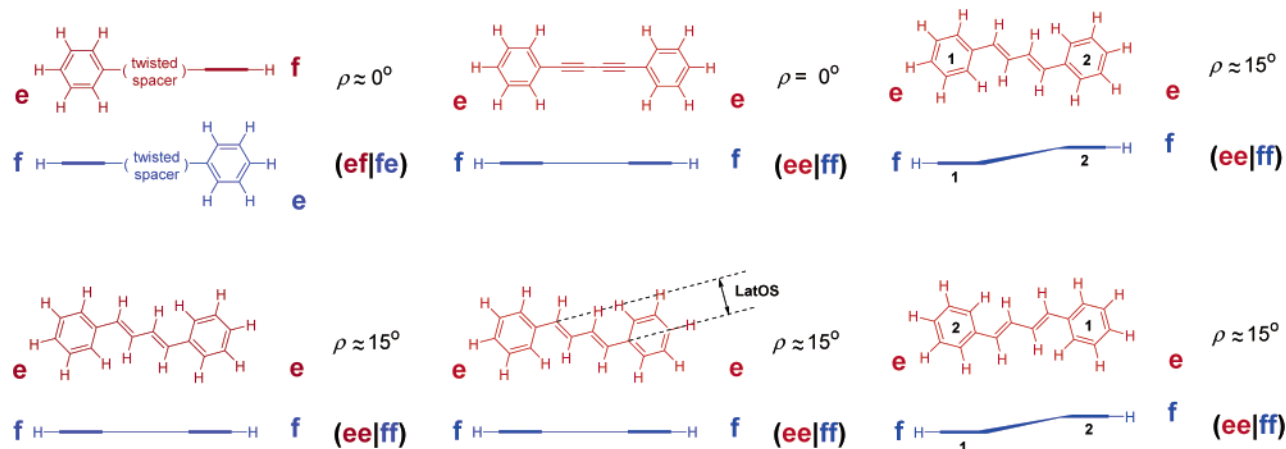


Figure 7. Schematic representation of the double T-contact (fe|ef) common in azines and of the new type of double T-contact (ff|ee) realized in 1,4-diphenylbutadiene. The (ff|ee) double T-contact between two different molecules causes diastereoisomeric contacts because each molecule can be either the (ee) or the (ff) component.

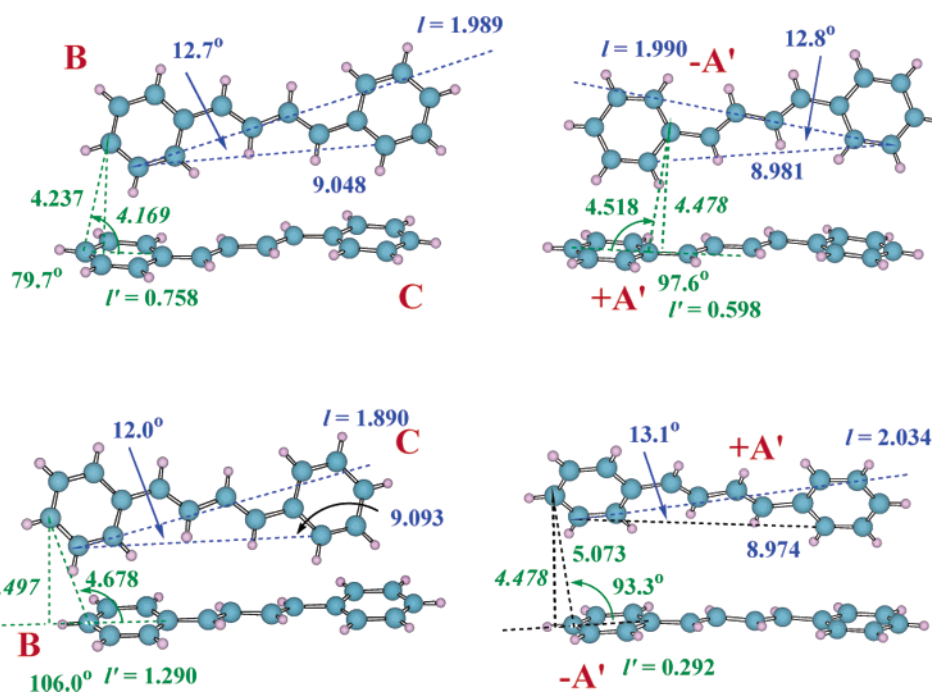
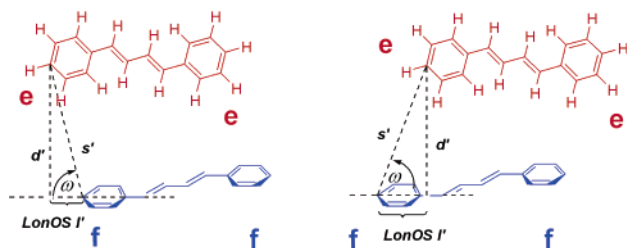


Figure 8. The four unique (ff|ee) double T-contacts in 1,4-diphenylbutadiene: +A'–A' (ff|ee), +A'–A' (ee|ff), BC (ee|ff) and BC (ff|ee). The values of ρ and s determine the lateral off-set l (blue). The values of ω and s' determine the longitudinal off-set l' (green) as well as the approach distance l' (green).

⊗ 3D rotatable images in PDB format of the four unique (ff|ee) double T-contacts in 1,4-diphenylbutadiene: ⊗ AA + (ff|ee), ⊗ AA – (ee|ff), ⊗ BC (ee|ff), and ⊗ BC (ff|ee) are available.

cases, C_{para} is closer to the (ff) molecule than is C_{ipso} . However, if C_{ipso} is closer then we use C_{ipso} instead of



$$\cos(\omega) = l' / s' \quad (\text{eq. 4})$$

$$\sin(\omega) = d' / s' \quad (\text{eq. 5})$$

C_{para} in otherwise analogous definitions (e.g., for the dimer on the top right in Figure 8). The longitudinal off-sets differ greatly with values from 0.6 up to 1.3 Å. The ω and s' data also can be used to characterize the stacking distances between the (ee) and (ff) molecules via the d value defined by eq 5. The d values for the BC contacts are 4.168 and 4.497 Å, and for the AA contacts they are 4.478 and 4.518 Å.

In Figure 9, we show sections of the layers of Figure 4 from different perspectives. To view the benzene rings edge-on, the columns in Figure 4 need to be rotated about the *horizontal* axis, and Figure 9 shows the results of this rotation for the (B, –A') and (C', +A') sets of columns. In the crystal, the molecules exhibit “wave-like” deformations. While subtle, these deformations are

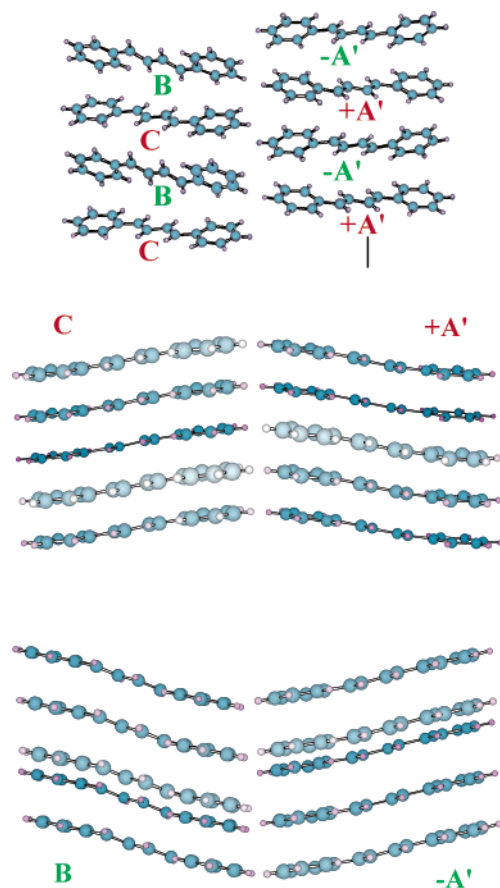


Figure 9. Side-views of the (B,-A') and (C,+A') sets of columns show a "wavelike" pattern. Color varies with depth.

⊗ 3D rotatable images of the ⊗ (B,-A'), and ⊗ (C,+A') sets of columns in PDB format are available.

clearly manifest, and the result of kinks between the C-Ph bonds and the best planes of the attached benzenes.

Interlayer Cooperation and Reduced Surface Matching. Benzene crystallizes in the space groups *Pbca*¹⁵ and *P2₁/c*.¹⁶ Several crystal structures were reported for each polymorph, and we employ the data of the CSD entries BENZEN and BENZEN04 in the present discussion. In Figure 10, we display the benzene structures and we show from top to bottom their layer arrangements (analogous to Figure 4), side views of the columns and layers (analogous to Figure 6 and including Figure 5), and the benzene dimers (analogous to Figure 8). Clearly, there is a close analogy in the crystal packings of **1** and of benzene itself. The layers in the *Pbca* structure of benzene are the same, but they are stacked such that every second layer is oriented the same. The interlayer contacts of **1** resemble the interlayer contacts of *P2₁/c* benzene (and considering A-C roughly the same).

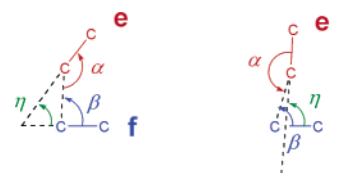
The major obvious difference between the benzene structures concerns the shape of the T-contact, and we use the angle η as a parameter to describe this feature. The angle η is defined by four benzene C atoms which are as much as possible in a common plane and in most cases the C_{meta} atoms are used. Results are summarized in Table 6. Three out of four η angles in **1** are within 1° of the angle of 60.5° in the *P2₁/c* benzene structure. Only the η value of 48.6° of the BC(ee|ff) contact is markedly

Table 6. Off-Set Values and Spacing Parameters

parameter	1	1	1	C ₆ H ₆ , <i>Pbca</i>	C ₆ H ₆ , <i>P2₁/c</i>
(ff ff)-contact	A	B	C		
δ	33.8	49.2	31.9	42.7	30.4
m	5.810	5.810	5.810	6.920	5.376
ParOS, p	4.828	3.796	4.933	5.086	4.637
SD, d	3.232	4.398	3.071	4.693	2.720
(ff ee)-contact	(-A +A)	(C B)	(B C)		
η^a	59.7	48.6 ^b	59.6	79.3	60.5
ρ	13.1	12.7	12.0		
s	8.974	9.048	9.093		
LatOS, l	2.034	1.989	1.890		
ω	93.3	79.8	106.0	76.5	79.8
s'	5.081	4.316	4.678	5.119	4.316
LonOS, l	0.292	0.758	1.290	1.195	0.764
SD, d'	5.073	4.169	4.497	4.978	4.248

^a Unless marked otherwise, the η values were determined based on the C_{meta} atoms in **1** and analogous in the benzenes. ^b This η value was based on the C_{ortho} atoms in the (ff) molecule and the C_{meta} atoms in the (ee) molecule.

lower. None of the η angles in **1** comes close to the respective value in the *Pbca* structure.



The immediate consequence of the near-perpendicular T-contact in the *Pbca* structure is the long stacking distance d in the face-to-face contacts. The stacking distance of $d = 4.7$ is about 2 Å longer than in the polymorph, and it is about 1.5 Å longer than for the face-to-face stacking distances between the A and C columns in **1**. Only the stacking distance $d = 4.4$ Å in the B columns comes close to the respective value in *Pbca* benzene. Suppose that the best T-contact is not the one that looks the most like a "T" and instead the best T-contact is one that looks like an italicized "T" or like a "7". Computations of benzene dimers support this view and it is likely to carry over to the solid. If this is true, then the B column's geometry is a winner because it realizes low η values and a high stacking distance $d = 4.7$. The T-contacts all are such that d' is larger than 4 Å irrespective of the η value.

To the left in Figure 11, the C_{para}-H groups on the surfaces of adjacent layers of *P2₁/c* benzene are shown. We connected the C atoms of the surfaces that are close to or far from the viewer, respectively, with unfilled and filled lines, respectively. One recognizes kite-shaped squares. These squares have direction in that the corner with the largest angle can be on the "right" or on the "left" and the shapes and their orientations are the same in the two layers—they match. The diagram on the right in Figure 11 is the analogous illustration for **1**. The occurrence of B molecules deforms the squares (along the green arrows) and they no longer are kite-shaped. The adjacent A layer adjusts to this deformation by becoming a (-A+A) layer with near-rhombic squares. In contrast, an (AA) layer would want to realize the kite-shaped squares, and any deviation in an effort to optimize interlayer interactions would raise the layer energy.

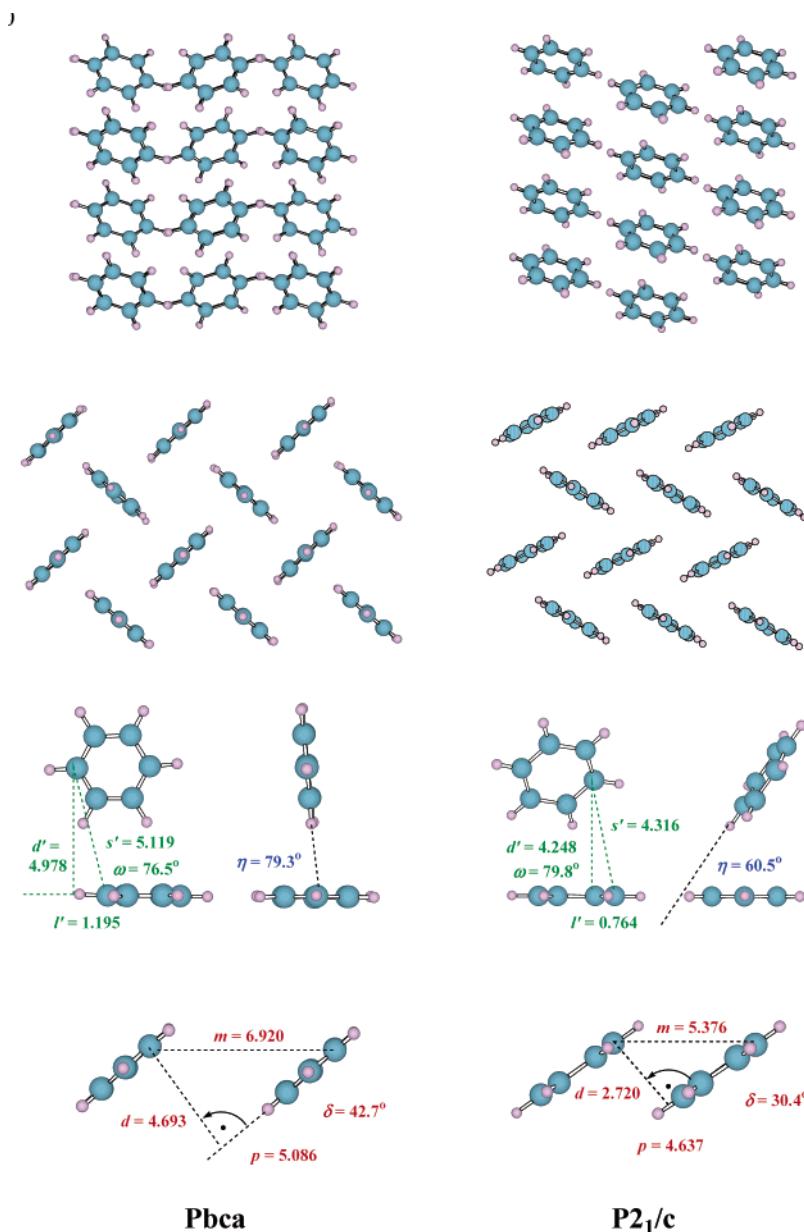


Figure 10. Crystal structures of benzene; *Pbc_a* on the left (BENZEN) and *P2₁/c* on the right (BENZEN04).

⊗ 3D rotatable structures of *Pbc_a* benzene (BENZEN, ⊗ crystal, ⊗ layer, ⊗ T-contact, ⊗ ff-contact) and of *P2₁/c* benzene (BENZEN04, ⊗ crystal, ⊗ layer, ⊗ T-contact, ⊗ ff-contact) in PDB format are available.

Conclusion

The crystal structure of 1,4-diphenylbutadiene contains three independent molecules A–C with modest *C_i* symmetric (or *C₇*-like) deformations due to twisting about the C–Ph bonds. The ab initio calculations show that the twisting in the crystal is much smaller than in the gas phase and only the B molecules show significant twisting. The deformations keep the best planes of the benzenes parallel (or almost parallel). Each molecule engages in two (ffff) double face-to-face contacts and in four (ee|ff) double T-contacts. Each molecule serves as the (ee) or (ff) molecule in two pairs of these (ee|ff) double T-contacts. These arene–arene interactions form two-dimensional layers and the layers are stacked in the third dimension and bound by van der Waals interactions.

We have shown that the arene–arene interactions in the crystal structure of 1,4-diphenylbutadiene are analogous to the *P2₁/c* structure of benzene. In addition, we have demonstrated that the crystal architecture of 1,4-diphenylbutadiene allows for more complex arene–arene interactions because the spacer-connected and laterally off-set dibenzene molecules allow for the formation of diastereoisomeric contacts. The two-dimensional layers can be formed with diastereoisomeric (ee|ff) double T-contacts either between two molecules of the same independent molecule (A) in two orientations (+A and –A) or between two independent molecules (B and C). Molecule A is asymmetric and forms enantiomeric (–A+A) and (–A'+A') layers. The alternation between layers with different pairs of diastereoisomeric double T-contacts allows for reduced surface-matching and improved van der Waals inter-

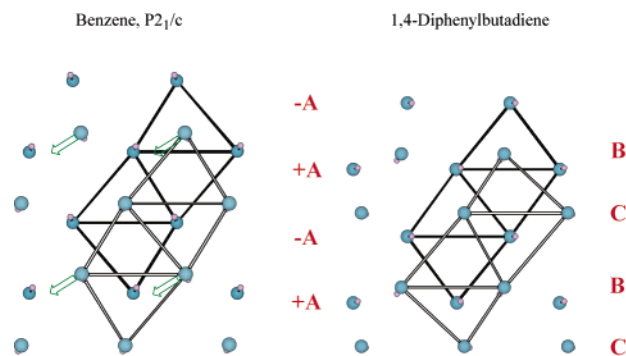


Figure 11. The surfaces are shown of adjacent layers for the $P2_1/c$ structure of benzene (left) and of **1**.

Ⓜ 3D rotatable images for the $P2_1/c$ structure of Ⓜ benzene and of Ⓜ **1** in PDB format are available.

actions between the surfaces of the $-A+A$ ($-A'+A'$) layers and the BC layers.

The crystal structure discussed is one of three known polymorphs, and our analysis suggests possible reasons for this polymorphism. One can imagine crystals formed by only one kind of layer with two diastereoisomeric (ee|ff) double T-contacts or by only one kind of layer with only one kind of (ee|ff) double T-contact. In addition, there might be layered structures with C_2 -distorted molecules and (ef|fe) double T-contacts, and there might be crystals without any of these layers. We hope to determine more of these polymorphs in future to advance our understanding of double arene–arene interactions.

Acknowledgment. This work was supported by the University of Missouri–Columbia Research Council and the MU Research Board. We thank MU Research Support Computing for generous allowances of computer time.

Supporting Information Available: Cartesian coordinates of the MP2(full)/6-311G** optimized C_h , C_2 , and C_{2h} symmetric structures and tables with details of the solid-state structure. This material is available free of charge via the Internet at <http://pubs.acs.org>.

References

- (1) *Anisotropic Organic Materials – Approaches to Polar Order*, Glaser, R., Kaszynski, P., Eds.; ACS Symposium Series, Vol. 798; American Chemical Society: Washington, DC, December 2001.
- (2) Steiger, D.; Ahlbrandt, C.; Glaser, R. *J. Phys. Chem. B* **1998**, *102*, 4257.
- (3) (a) Lewis, M.; Barnes, C. L.; Glaser, R. *J. Chem. Crystallogr.* **2000**, *30*, 489. (b) Lewis, M.; Barnes, C.; Glaser, R. *Acta Crystallogr. C* **2000**, *56*, 393. (c) Chen, G. S.; Wilbur, J. K.; Barnes, C. L.; Glaser, R. *J. Chem. Soc., Perkin Trans. 2* **1995**, 2311.
- (4) Lewis, M., Ph.D. Dissertation, University of Missouri–Columbia, 2001.
- (5) (a) Lewis, M.; Glaser, R. *J. Org. Chem.* **2002**, *67*, 1441. (b) Glaser, R.; Lewis, M.; Wu, Z. *J. Mol. Model.* **2000**, *6*, 86. (c) Glaser, R.; Chen, G. S. *J. Comput. Chem.* **1998**, *19*, 1130.
- (6) (a) Sauro, V. A.; Workentin, M. S. *J. Org. Chem.* **2001**, *66*, 831. (b) Zuman, P.; Ludvik, J. *Tetrahedron Lett.* **2000**, *41*, 7851. (c) Riedl, F.; Ludvik, J.; Liska, F.; Zuman, P. *J. Heterocycl. Chem.* **1996**, *33*, 2063. (d) Ludvik, J.; Riedl, F.; Liska, F.; Zuman, P. *J. Electroanal. Chem.* **1998**, *457*, 177. (e) Lund, H. *Acta Chem. Scand.* **1959**, *13*, 249.
- (7) Lewis, M.; Wu, Z.; Glaser, R. In *Anisotropic Organic Materials – Approaches to Polar Order*, Glaser, R., Kaszynski, P., Eds.; ACS Symposium Series, Vol. 798; American Chemical Society: Washington, DC, 2001; Chapter 7, p 97.
- (8) Hengstenberg, J.; Kuhn, R. *Z. Krist.* **1930**, *75*, 301.
- (9) Drenth, W.; Wiebenga, E. H. *Recueil.* **1953**, *72*, 39.
- (10) (a) Cramer, C. J. *Essentials of Computational Chemistry, Theories and Models*, John Wiley & Sons: Chichester, UK, 2002. (b) Hehre, W. J.; Radom, L.; Schleyer, P. R.; Pople, J. *Ab Initio Molecular Orbital Theory*, John Wiley & Sons: New York, 1986.
- (11) Gaussian 98: Frisch, M. J.; Trucks, G. W.; Schlegel, H. B.; Scuseria, G. E.; Robb, M. A.; Cheeseman, J. R.; Zakrzewski, V. G.; Montgomery, J. A., Jr.; Stratmann, R. E.; Burant, J. C.; Dapprich, S.; Millam, J. M.; Daniels, A. D.; Kudin, K. N.; Strain, M. C.; Farkas, O.; Tomasi, J.; Barone, V.; Cossi, M.; Cammi, R.; Mennucci, B.; Pomelli, C.; Adamo, C.; Clifford, S.; Ochterski, J.; Petersson, G. A.; Ayala, P. Y.; Cui, Q.; Morokuma, K.; Malick, D. K.; Rabuck, A. D.; Raghavachari, K.; Foresman, J. B.; Cioslowski, J.; Ortiz, J. V.; Baboul, A. G.; Stefanov, B. B.; Liu, G.; Liashenko, A.; Piskorz, P.; Komaromi, I.; Gomperts, R.; Martin, R. L.; Fox, D. J.; Keith, T.; Al-Laham, M. A.; Peng, C. Y.; Nanayakkara, A.; Challacombe, M.; Gill, P. M. W.; Johnson, B.; Chen, W.; Wong, M. W.; Andres, J. L.; Gonzalez, C.; Head-Gordon, M.; Replogle, E. S.; Pople, J. A. *Gaussian 98*, Revision A.9, Gaussian, Inc., Pittsburgh, PA, 1998.
- (12) Parent butadiene structure: (a) Wiberg, K. B.; Rosenberg, R. E.; Rablen, P. R. *J. Am. Chem. Soc.* **1991**, *113*, 2890. (b) Wiberg, K. B.; Rosenberg, R. E. *J. Am. Chem. Soc.* **1990**, *112*, 1509.
- (13) Nakano, K.; Sada, K.; Kurozumi, Y.; Miyata, M. *Chem. Eur. J.* **2001**, *7*, 209.
- (14) (a) Hobza, P.; Selzle, H. L.; Schlag, E. W. *Chem. Rev.* **1994**, *94*, 1767. (b) See ref 7 and references cited therein for details.
- (15) (a) BENZEN and BENZEN01 (neutron diff.): Bacon, G. E.; Curry, N. A.; Wilson, S. A. *Proc. R. Soc. London, Ser. A* **1964**, *279*, 98. (b) BENZEN02: Cox, E. G.; Cruickshank, D. W. J.; Smith, J. A. S. *Proc. R. Soc. London, Ser. A* **1958**, *247*, 1. (c) BENZEN05: Weir, C. E.; Piermarini, G. J.; Block, S. *J. Chem. Phys.* **1969**, *50*, 2089.
- (16) (a) BENZEN03: Piermarini, G. J.; Mighell, A. D.; Weir, C. E.; Block, S. *Science* **1969**, *165*, 1250. (b) BENZEN04: Fourme, R.; Andre, D.; Renaud, M. *Acta Crystallogr., Sect. B* **1971**, *27*, 1275.

CG034006M